Impulse Testing of Corporate-Fed Patch Array Antennas

Neil F. Chamberlain
Jet Propulsion Laboratory
California Institute of Technology
4800 Oak Grove drive
Pasadena, CA 91109
818-354-7879
Neil.F.Chamberlain@jpl.nasa.gov

Abstract—This paper discusses a novel method for detecting faults in antenna arrays. The method, termed *Impulse Testing*, was developed for corporate-fed patch arrays where the element is fed by a probe and is shorted at its center. Impulse Testing was devised to supplement conventional microwave measurements in order to quickly verify antenna integrity. The technique relies on exciting each antenna element in turn with a fast pulse (or impulse) that propagates through the feed network to the output port of the antenna. The resulting impulse response is characteristic of the path through the feed network. Using an oscilloscope, a simple amplitude measurement can be made to detect faults. A circuit model of the antenna elements and feed network was constructed to assess various fault scenarios and determine fault-detection thresholds. The experimental setup and impulse measurements for two patch array antennas are presented. Advantages and limitations of the technique are discussed along with applications to other antenna array topologies[1,2].

TABLE OF CONTENTS

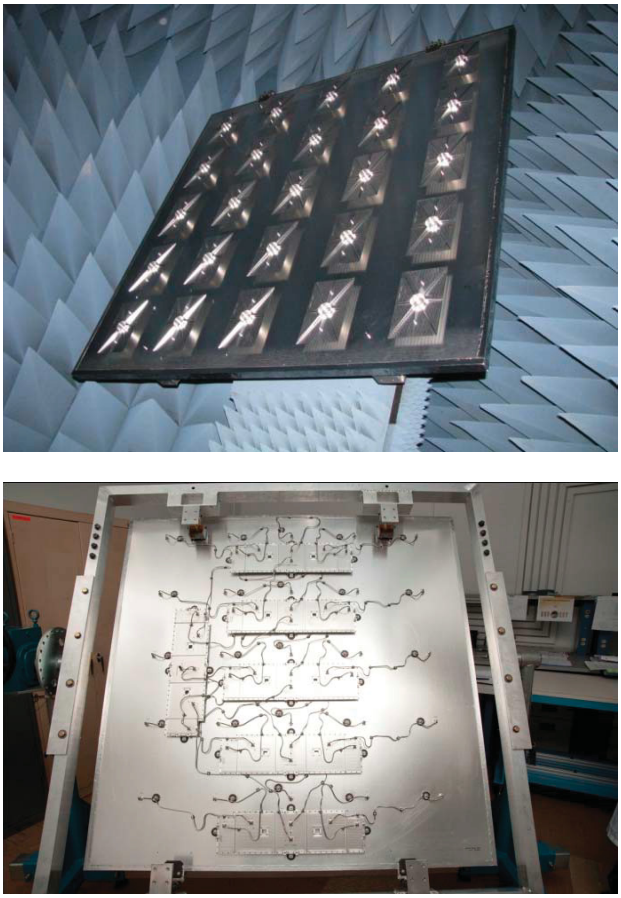

Figure 1 – Antenna construction for Juno MWR A1 Front showing antenna elements (top), back showing feed network (bottom)

1. INTRODUCTION

This paper introduces a new method of testing corporate-fed patch array antennas. The test involves propagating a fast pulse through the antenna to verify continuity in the feed network interconnects and circuits. Impulse Testing was conceived as a quick and reliable method of testing the Juno Microwave Radiometer (MWR) antennas before and after environmental tests (or other procedures) that might potentially damage the hardware. By comparing the results of 'before' and 'after' Impulse Tests, one can obtain a high degree of confidence that the antenna has not been damaged as a result of testing or handling. Impulse Testing is not intended to replace conventional techniques, such as pattern measurements and impedance measurements, to verify RF performance. Rather, it is intended as a verification / diagnostic tool in the same way that a continuity checker is used to verify connectivity in an electronic circuit. It has the advantage of being quick, requires simple low-cost test equipment, and can be performed in confined spaces, such as an environmental test chamber. As the measurement is made sequentially at each antenna element, it is possible to isolate a fault path and further troubleshoot a potential anomaly. This paper develops the theory of Impulse Testing

[1] 978-1-4244-7351-9/11/$26.00 ©2011 IEEE
[2] IEEEAC paper #1741, Version 3, Updated January 9, 2011

through a circuit model that closely emulates measurements. The model is used to test various fault scenarios, and from these results an understanding of the capabilities (and limitations) of Impulse Testing is inferred. An Impulse Test procedure and measured Impulse Test data for MWR patch array antennas are also presented.

The Juno MWR A1 and A2 antennas are patch array antennas that operate at 600 MHz and 1250 MHz respectively. The antennas share a common architecture and construction approach (Figure 1 and Figure 2) that results in hardware having thousands of parts and hundreds of interconnects. Specifically, there are 194 solder joints and 30 male-female coaxial interfaces in the feed network of each antenna. These protoflight antennas have stringent electrical and environmental performance requirements that are verified though a sequence of RF, thermal, and acoustic testing.

The test sequence, which is typical for many flight antenna systems, involves bracketing the environmental tests with pattern measurements and impedance measurements. The intent of this test plan is to measure the RF performance of the antennas and at the same time ensure that the antennas are not damaged by environmental testing. Typically, intermediate impedance measurements (reflection coefficient or return loss) are made between successive environmental tests to further assure antenna integrity. A reflection coefficient measurement is an aggregate of all the reflected signals in the antenna and its scattering environment. Therefore for some antenna configurations, a fault in the interconnect network may not necessarily manifest as a perceptible change in the reflection coefficient characteristic; especially if the measurements are improvised in an environmental testing chamber.

The A1 and A2 antenna feeds are designed with Wilkinson power divider circuits that provide reasonably high isolation between elements. Consequently, an open-circuit or short-circuit in the feed network does not necessarily show up as a poor match at the antenna output, because the reflected energy tends to dissipate in one or more of the isolation resistors. This was precisely the case for the MWR A2 antenna, where the return loss was measured with a cable accidentally disconnected at one power divider, and was judged to be 'good' (compared favorably with predictions). It was only after the antenna pattern was measured that the issue was discovered and later corrected. Measurement of antenna patterns after each environmental test is normally not feasible for cost and schedule reasons, and re-measurement of the feed network S-parameters would involve disconnecting cables which would pose an unacceptable risk to flight hardware. As a consequence, the Impulse Test was developed to address the issue of assuring antenna integrity.

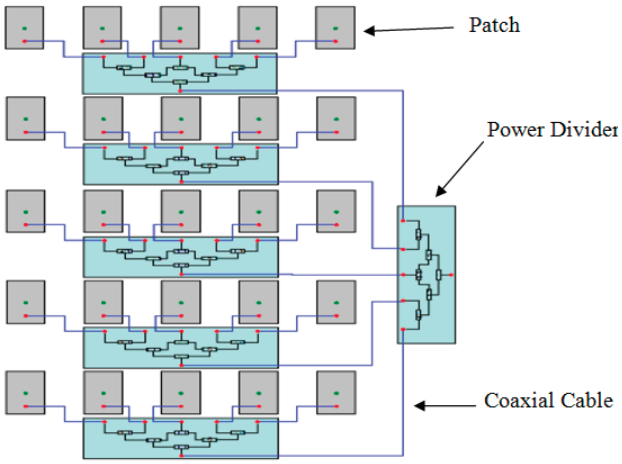

Figure 2 – Antenna Architecture for A1 antenna and A2 antenna showing 5-way power dividers connected to patch elements through coaxial cables

2. THEORETICAL DEVELOPMENT

This section develops the theoretical basis and understanding of the Impulse Test through a circuit model that closely emulates the impulse response of the A1 and A2 antennas. These circuit models will be used to test likely fault scenarios in order to assess the capabilities (and limitations) of Impulse Testing. The analysis starts with the development of a low-frequency circuit model for the A1 metal patch antenna. A simplified version of this patch circuit model is then incorporated into a circuit model representing the full A1 antenna. A mixture of frequency-domain and time-domain techniques is utilized for this purpose. The Impulse Test is naturally a time-domain method, but the available software required the use of frequency-domain tools. The approach for the A2 antenna is identical and is therefore not elaborated.

The formulation of a circuit-model for Impulse Testing begins with the formulation of a simple circuit model for the patch itself. The patch element can be viewed as a shorted microstrip transmission line. The impedance (ohm) of the free-standing patch is defined as [1]

$$Z_0 = \frac{120\pi}{\sqrt{\varepsilon}[W/H + 1.393 + 0.667\ln(W/H + 1.444)]} \qquad (1)$$

For the dimensions of MWR A1 (Figure 3) Z_0 is 39.4 ohms (ε, the effective permittivity is 1 for a metal patch). There is a hole in the patch beneath the pedestal that reduces the area by 5%. To first order, this will increase the impedance by 5% so the equivalent patch impedance is 41.3 ohms. From this value of patch impedance, values of inductance and capacitance may be derived as follows:

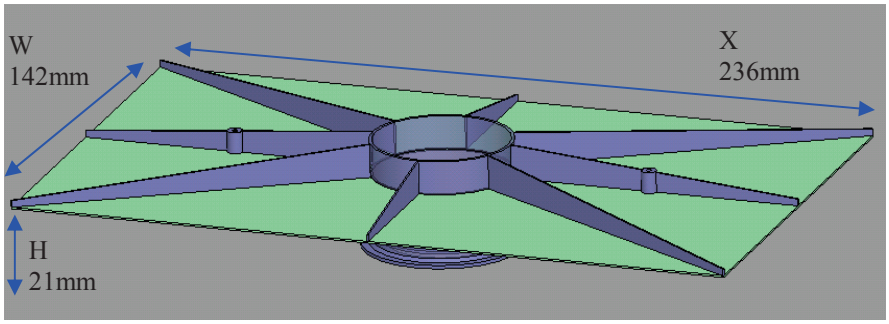

Figure 3 – MWR A1 metal patch and dimensions

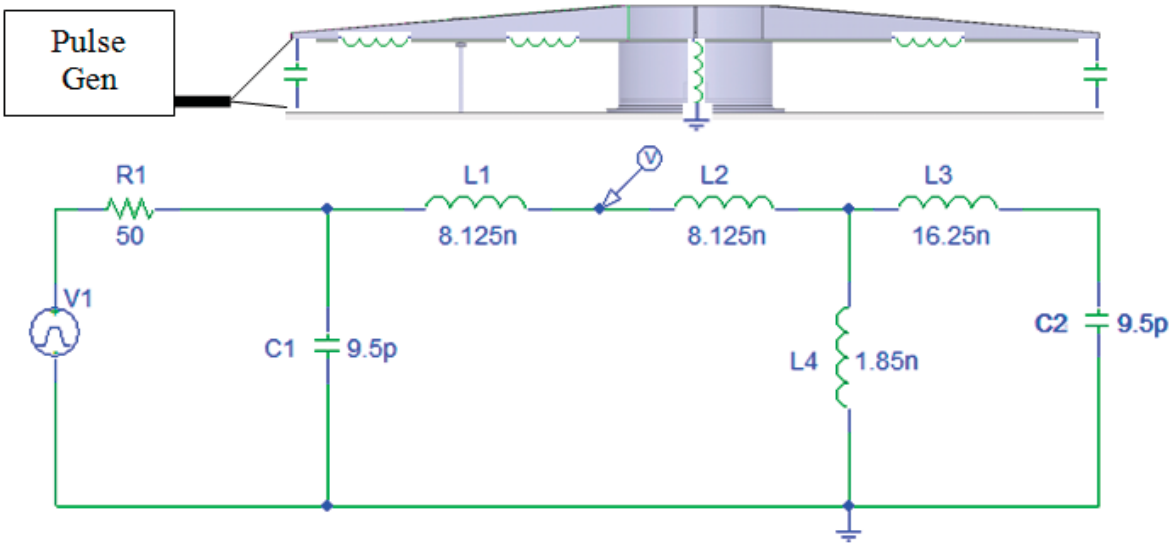

Figure 4 – Circuit model for MWR A1 patch and pulse generator. The patch connects to the antenna feed network at the node L1-L2.

$$L = Z_0 / v = 138\,nH/m$$
$$C = 1/(Z_0 v) = 81\,pF/m$$

where v is the velocity of the wave propagating in the line. The inductance and capacitance of the patch are calculated by taking the above per-length values, respectively, and multiplying them by the patch length X (which is 236 mm for A1)

$$L_{patch} = XZ_0 / v = 32.5\,nH$$

$$C_{patch} = X/(Z_0 v) = 19\,pF$$

The pedestal inductance can be calculated (from [2]) as follows:

$$\mathrm{L_{ped}} = 2\mathrm{H}[\ln(2\mathrm{H}/\mathrm{D}(1+\mathrm{x})) - \mathrm{x} + \mathrm{D}/(2\mathrm{H})]$$
$$x = \sqrt{1+(1+D/(2H))^2}$$

where H is the length of the pedestal (i.e., height of patch) in cm. This is a high-frequency solution because it does not include an internal inductance component; it assumes that the current in the pedestal lies principally on the surface and that no magnetic flux is internal to the conductor. This yields a pedestal inductance of 1.85nH.

Using these values, the patch model indicated in Figure 4 is formulated. The output impedance of the signal generator is modeled as a 50 ohm resistor R1. The pulse generator V1 has an open circuit peak voltage of 10 volts in order to deliver a peak voltage of 5V matched to a 50 ohm load. The voltage levels are not critical, but should be sufficient to allow measurement at the output of the antenna and not damage it. The pulse generator V1 has a rise-time of 5 ns. The rise-time determines the duration of the excitation pulse by virtue of the differentiating nature of the input circuit. A 5ns pulse (for this application) represents a good compromise between good temporal resolution (narrower pulse) and exciting the feed network below its normal operating frequency (wider pulse). Fall-time, pulse length and period are not critical parameters. The pulse should be

long enough that the trailing edge occurs after the impulse response has died out. In the subsequent simulations and measurements, the fall-time, pulse length and period are set to 5ns, 20µs, and 1ms respectively.

The signal generator connects to the patch by means of an open coaxial cable. This probe assembly has a small sense inductance of about 1nH, but this detail is omitted from the model, as it has little impact. The 32.5nH of patch inductance is distributed among L1, L2 and L3. L4 represents the pedestal inductance. The feed point of the patch ('v' symbol in Figure 4) is roughly a quarter of the length of the patch from the end, hence the partitioning of patch inductance. Since the patch is being excited below its normal operating frequency, the radiation resistance of the patch need not be incorporated into the model. The feed impedance is not incorporated in the model at this point

The pulse response of the circuit in Figure 4 is shown in Figure 5. The red trace corresponds to the voltage generated by the coaxial probe connected to the signal generator (R1-C1 in Figure 4) and the green trace corresponds to the signal at the patch feed point. It is this signal that propagates through the feed network to the output. The corresponding power spectrum for the (green) input pulse is also shown in Figure 5. The first null at 200MHz is calculated as the inverse of the pulse duration, 5ns. Approximately 90% of the energy of the pulse is below the MWR A1 band, with the majority of it at 100MHz and below.

Operating below the normal operating frequency has the advantage that inter-patch coupling is reduced, making the test much more dependent on the path from a particular patch through the feed network to the output. Inter-patch coupling is shown in Figure 6 for the center element and vertically adjacent elements (which are the most strongly coupled). Near the operating band, patch coupling is as high as -12 dB, whereas at 200 MHz, the coupling is -56 dB. Since the impulse response path loss is on the order of 10dB (at the pulse frequency band), pulse propagation favors the feed network as opposed to patch-to-patch coupling.

To simplify subsequent modeling and aid understanding, the model in Figure 4 is reduced to the model shown in Figure 7. The antenna input circuit (not including the feed) is seen as a 10nH inductor in parallel with a 5pF capacitor. These values were derived empirically. The resulting pulse excitation waveform for this circuit is shown in Figure 7.

At 200MHz, the reactance of the inductor is 12ohms, whereas the reactance of the capacitor is 159ohms, so the inductor dominates the input impedance of the patch (neglecting the feed) and (in tandem with the signal generator output resistance) serves to differentiate the pulse of the signal generator. The capacitance contributes to the modest oscillatory nature of the waveform.

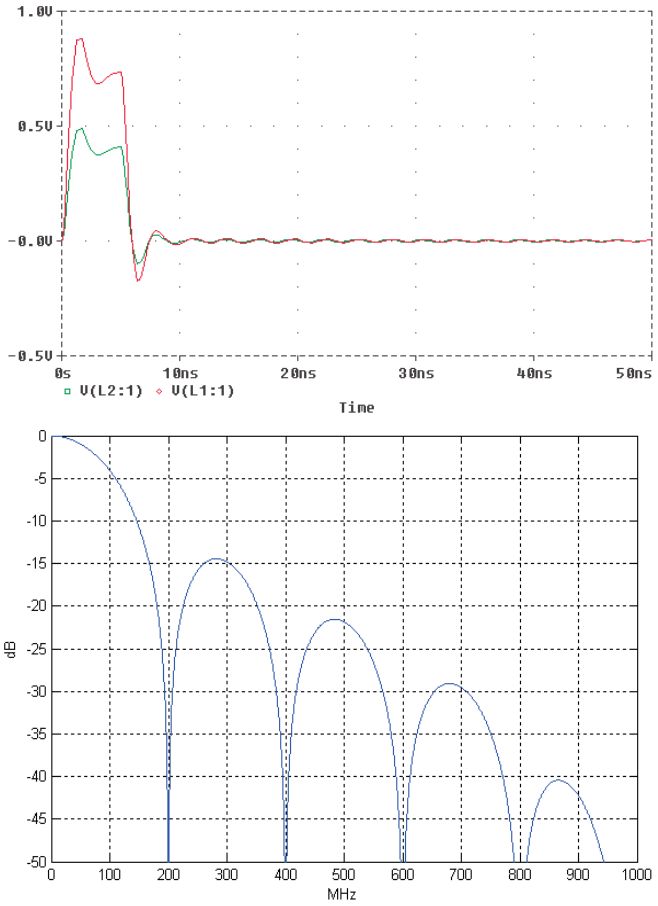

Figure 5 – Pulse response (top) and spectrum (bottom) for circuit of Figure 4

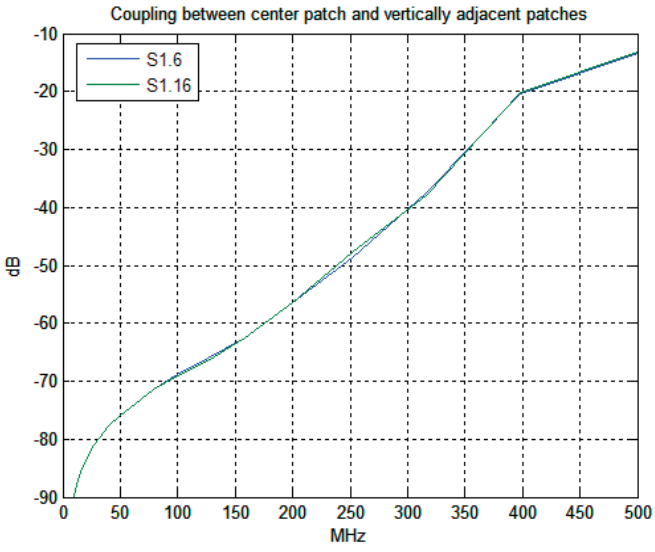

Figure 6 – Inter-patch coupling of A1 antenna as a function of frequency

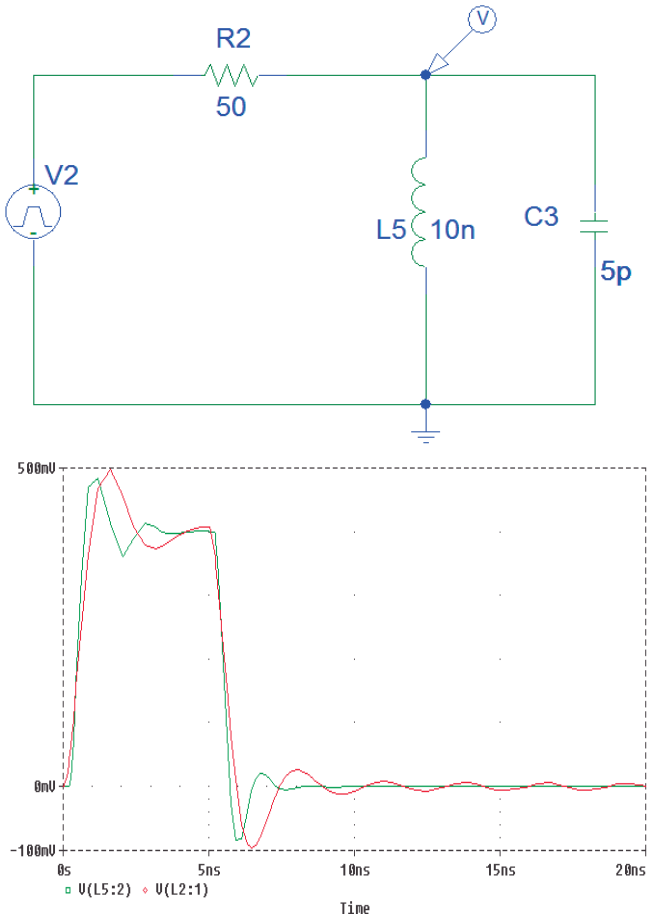

Figure 7 – Top: simplified model for MWR A1 patch and pulse generator. Bottom: pulse response of simplified input circuit model (green curve), pulse response of circuit in Figure 4 (red curve).

In summary, when a 5V amplitude, 5ns rise-time rectangular pulse is applied to the edge of an A1 metal patch (near the probe end of the patch), the input circuit serves to differentiate the leading edge (and also trailing edge), coupling a pulse of approximately +0.5V amplitude and 5ns width to the antenna feed network. As will be shown next, this pulse propagates through the feed network, primarily through the direct path from patch to output, but also reflecting from the various transmission line interfaces of the feed.

Antenna Array Model

A circuit model for the MWR A1 antenna is shown in Figure 8. This model was constructed in Ansoft Designer. The model comprises lumped circuit elements and lossy transmission lines with parameters set to emulate the coaxial cables and stripline transmission lines of the 5-way power dividers. The antenna patches are modeled as an inductor in parallel with a capacitor, as previously described. A sinusoidal signal source is connected to the patch circuit model through a 50ohm transmission line. The oscilloscope is modeled as a 1Mohm resistor in parallel with 13pF capacitor.

A linear frequency synthesis is performed over the band 0 to 1GHz for 2501 points. The data are ported to MATLAB, where the data are first converted to the time-domain using the Fast Fourier Transform and are then multiplied by the frequency response of the 5ns pulse and a 100MHz low-pass filter to emulate the frequency response of the oscilloscope. The time-domain data points have 1ns resolution and 2.5μs extent. The impulse response to the circuit of Figure 8 is shown in Figure 9 along with measured data for the A1 antenna for comparison. While these curves are not exact overlays of each other, they are comparable in terms of signal level, latency, decay rate, and overall appearance. The indicated peak voltages are typical of the range measured for MWR A1, namely 100mV to 165mV, depending on the particular element. The voltages are strongest at center-most elements, but the amplitude variation is less pronounced than the Taylor pattern taper at 600MHz.

The time constant of the signal is about 250ns and is heavily influenced by 1 M ohm load oscilloscope resistance. Using the 50 ohm setting on the oscilloscope would result in a shorter output pulse because the 50 load represents a better match to the feed network. The ringing in this case dies out to zero in about 200 ns. However, the use of a high-impedance load at the oscilloscope input increases the amount of energy echoing back and forth in the feed network and enhances the chance of detecting a defect.

To further simplify the Impulse Test model in order to gain insight into its operation, the circuit in Figure 9 is reduced to the model shown in Figure 10. T10 is a lossy transmission line with the same delay as the MWR A1 feed network (12 ns) and the cable attaching A1 to the oscilloscope (8 ns). The corresponding output waveform is shown in Figure 11 and very roughly approximates previous waveforms. The period of this waveform (40ns) is twice the delay from input to output (20ns), and the decay rate is determined by the attenuation in the various transmission lines. The measured impulse responses are essentially a superposition of the waveform shown in Figure 11.

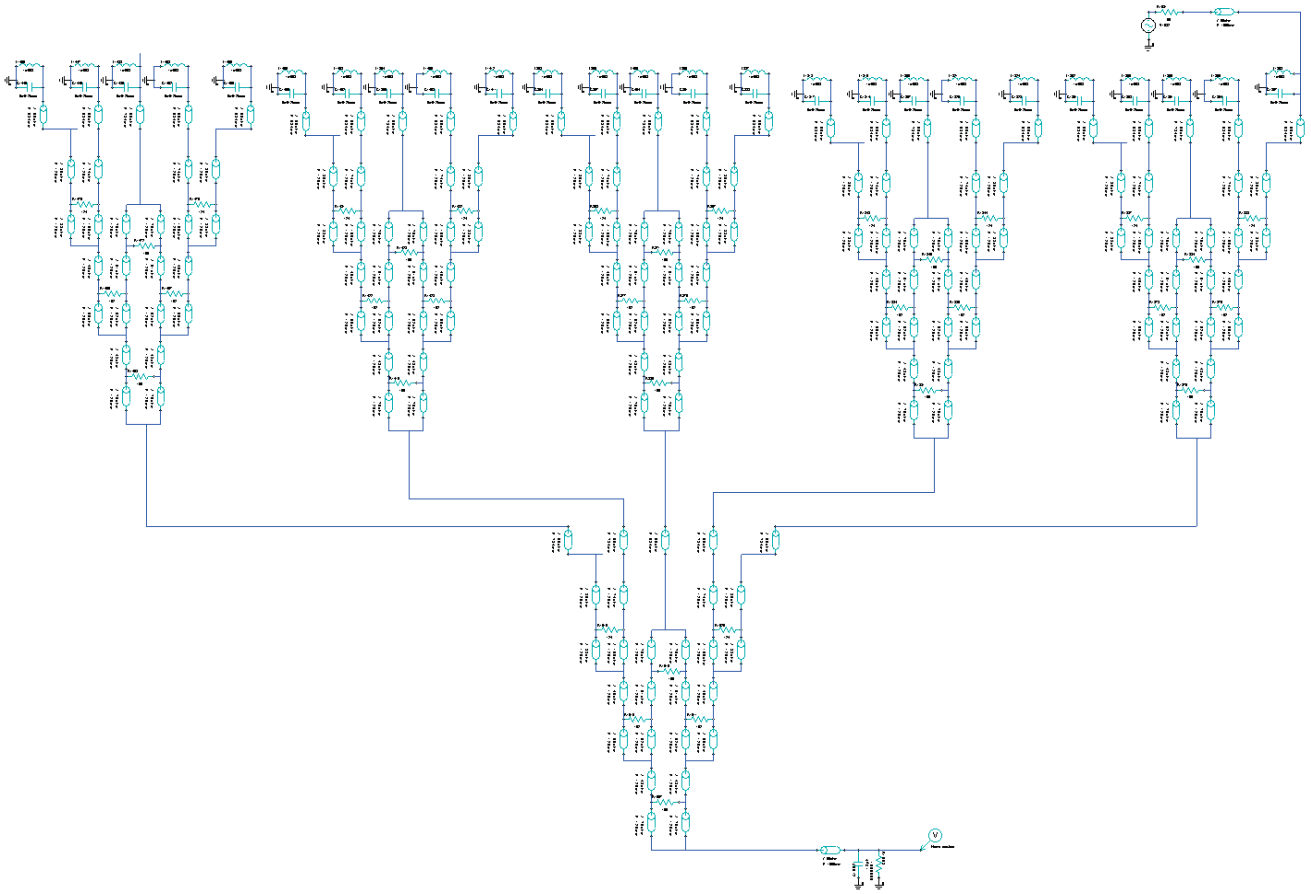

Figure 8. MWR A1 antenna Impulse Test Designer model

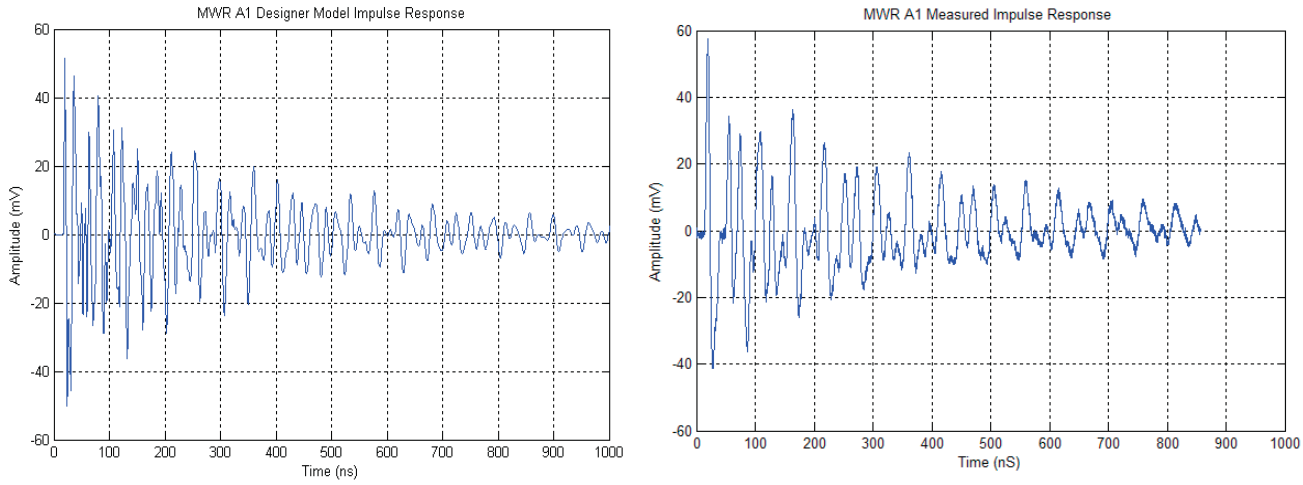

Figure 9 – Pulse response of circuit model (left) compared to measured data for MWR A1 (right). Measured data record terminates at 850 ns

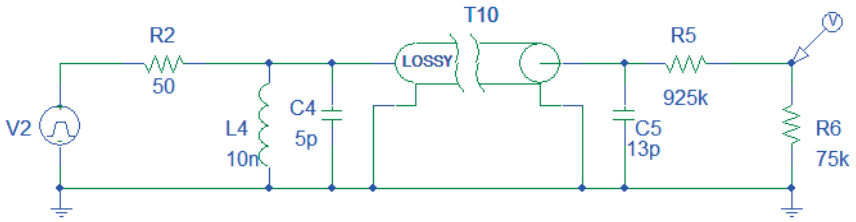

Figure 10 – Simplified MWR A1 Impulse Test Spice model

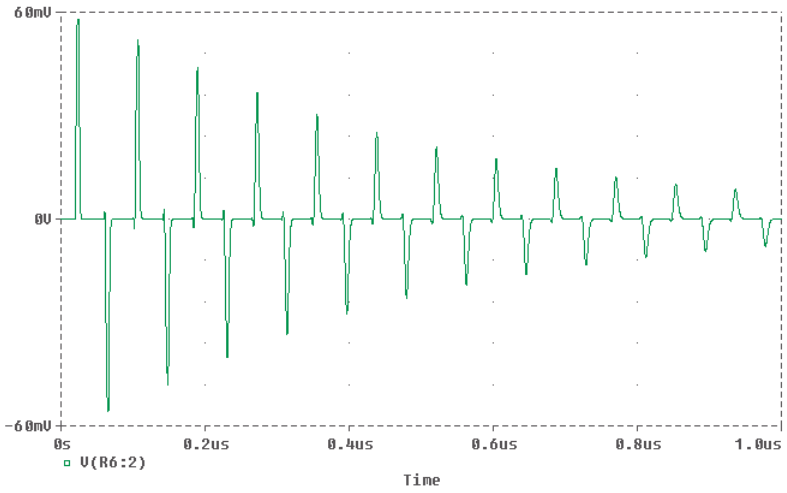

Figure 11 – Pulse response for circuit in Figure 10

3. Fault Scenarios and Detection Criteria

Because it is generally difficult to experiment with flight hardware, the following investigation of fault scenarios focuses on the circuit model of Figure 8. This is a limited (i.e., non-exhaustive) investigation of the waveforms that result when various fault conditions are manifested in the feed network. Open-circuits represent the most likely 'catastrophic' fault scenarios. In the MWR hardware, this could arise as a result of power divider ribbon detachment or coaxial cable center pin detachment. Short-circuits are also possible but less likely. For example an interconnect ribbon could detach from the circuit board and short against a probe sleeve. Isolation resistor detachment can also be investigated by removing resistors from the model. Finally, another class of faults that can be detected is the partial detachment of metal patch. This causes the input inductance (L4 in Figure 4) to increase with a corresponding increase in the output voltage.

An open circuit is modeled as an ideal capacitance of 1.5pF, and a short circuit is modeled at an inductance of 1.5nH. These circuit values correspond to a reactance of approximately 500ohm and 2ohm, respectively, at 200MHz (the nominal band containing most of the energy of the resonating pulse). These impedances are an order of magnitude different than the typical transmission line impedances in the feed network, which range from 36ohm to 159ohm.

Figure 12 shows the impulse response to different open circuit and short circuit fault scenarios in the feed network. Figure 13 shows the impulse response to different detached resistor scenarios in one path of the feed network. These results show that in all cases the pulse voltage at the output of the antenna is reduced significantly; typically by a factor of 5, but at least a factor of 2. From these results, and measurements that are discussed in the next section, a simple qualitative pass-fail test criterion can be derived:

If the measured impulse voltage increases or decreases by more than 50% from nominal, one should suspect a fault and investigate further.

Conversely, if the measured peak impulse voltages fall within ±50% of the nominal and the return loss measurements have reasonable agreement (judged relative to the scattering environment of the measurement), then it is likely - but not guaranteed - that the antenna is fault free.

In some cases, the waveform shape is quite different to the waveforms in Figure 12. As an addendum to the above criterion, a more qualitative criterion can be formulated in terms of the similarity of wave shape. However, this does require judgment on behalf of the operator.

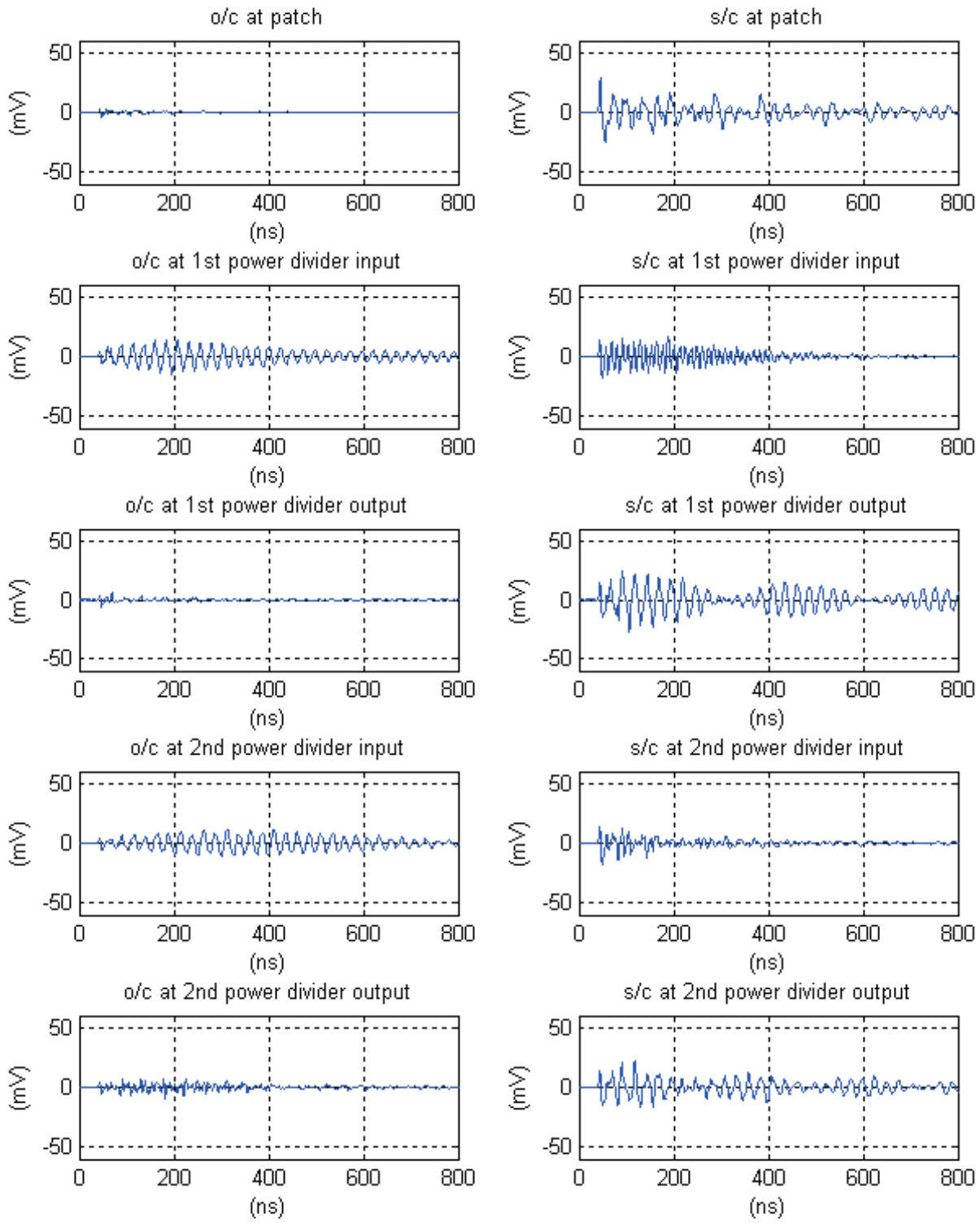

Figure 12 – Impulse responses to various open circuit and short circuit fault scenarios. In all cases the peak output voltage is reduced by 50% or more compared to the fault-free condition

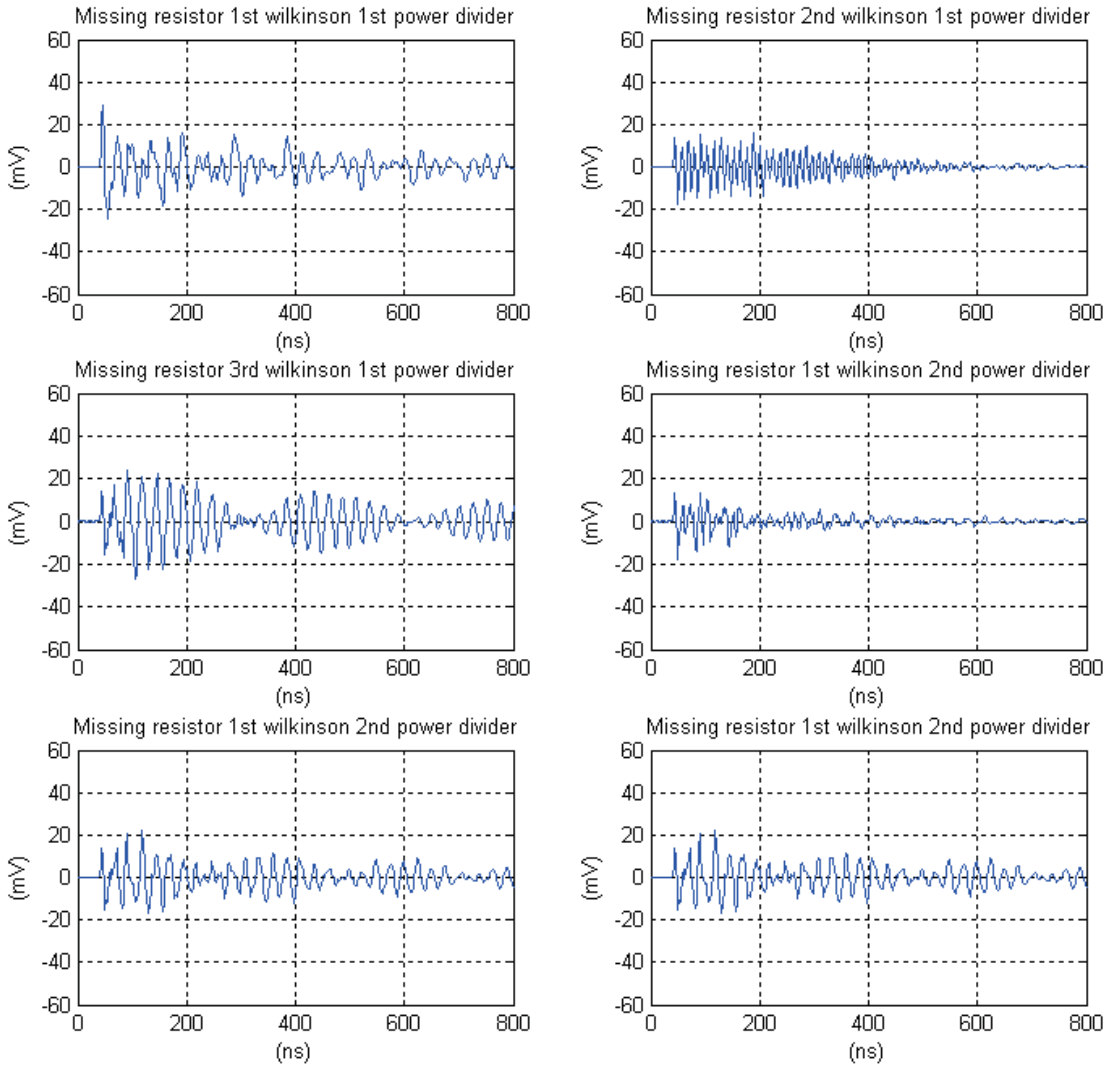

Figure 13 – Impulse responses to various missing resistor fault scenarios. In all cases (with the possible exception of the first) the peak output voltage is reduced by 50% or more compared to the fault-free condition

In the case of a partially attached metal patch, the base impedance will increase compared to its value when the patch is properly seated. Therefore a partially detached metal patch will be detected by the above criteria if the inductance increased by more than 50%. Improperly seated A2 metal patches had pulse responses that were many times the nominal value.

The next section discusses the measurement setup for Impulse Test and measurements on the A1 and A2 antennas.

4. TEST SETUP AND EXPERIMENTAL RESULTS

The Impulse Test setup for the A1 FM antenna is shown in Figure 14. A pulse generator is used to generate a fast pulse that is coupled to the patch element using a custom coaxial probe. This generator should have the ability to control rise time. The output of the A1 antenna is connected to Channel 1 of a sampling oscilloscope. The oscilloscope is synchronized through Channel 2 by the signal generator 'sync' signal. The oscilloscope is connected to measure the signal at the output of the antenna on Channel 1 due to a pulse excited at each of the patches in turn. An oscilloscope with bandwidth of 100MHz or more is sufficient for this purpose, although a digital oscilloscope with waveform capture (or hold) and waveform measurement capability is convenient for the present application. Peak-to-peak amplitudes are captured by the oscilloscope in subsequent measurements. As the probe is an open-ended coaxial cable, the probe coupling is set to 1X (times 1) AC. The resulting impulse responses will depend on the particular antenna configuration – for the A1 and A2 antennas an amplitude scale of 20mV/div and 10mV/div were used, respectively. The time scale was set to 100ns/div for both antennas. The pulse generator should have an adjustable pulse width,

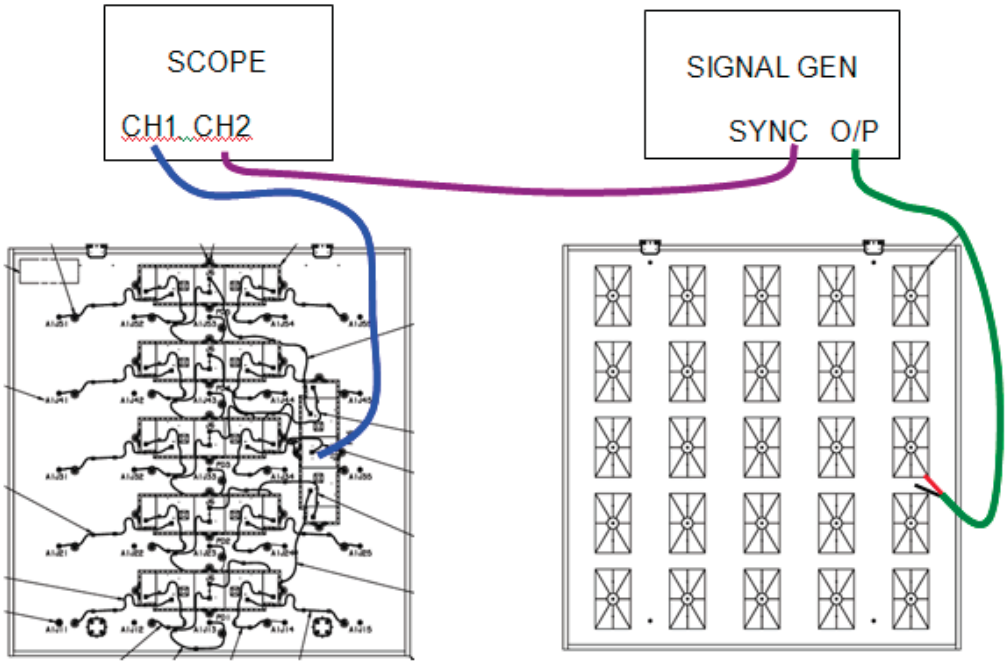

Figure 14 – Impulse Test setup for A1 antenna

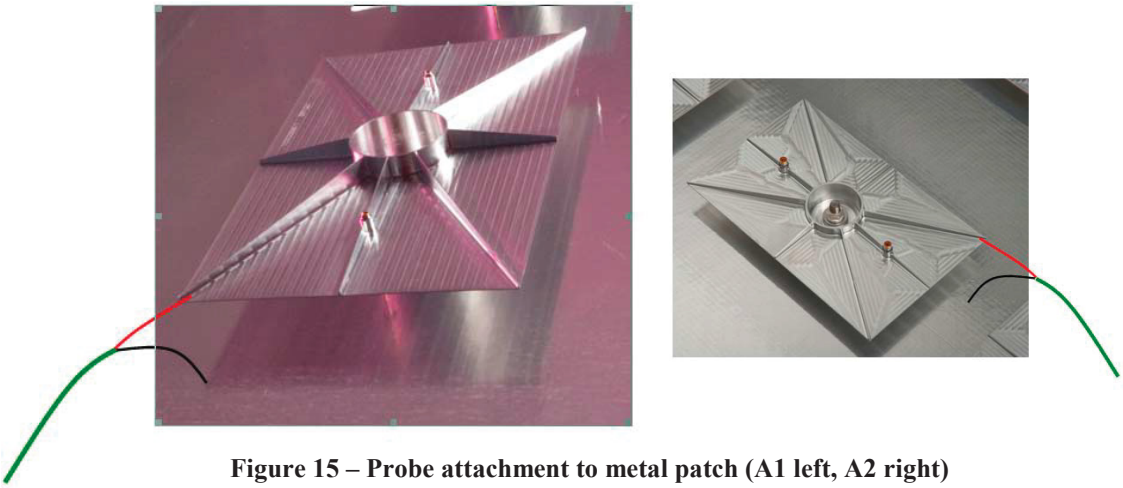

Figure 15 – Probe attachment to metal patch (A1 left, A2 right)

frequency, and rise-time. These variables were set to 20us, 1kHz, and 5ns, respectively for both the A1 and A2 antennas. The values will need to be adjusted for other configurations; particularly the pulse width to ensure that successive impulse responses (one from the leading edge and one from the trailing edge) do not overlap. A square pulse with 5V peak amplitude was used in subsequent measurements. It should also be noted that by virtue of the differentiating nature of the input circuit, excitation pulse amplitude will also depend on the pulse rise-time.

A 'custom' coaxial probe (Figure 16) is attached to the corner of the patch nearest the feed point, as indicated in Figure 15. The probe is simply an SMA terminated coaxial cable of approximately 6" length with the non-terminated end cut and stripped to reveal the center conductor and ground sheath. The ground sheath and exposed center conductor are long enough to form a loop of approximately 0.5" diameter. The dimensions are not critical but should generally be kept small consistent with the need to make contact with the patch and the antenna ground plane. It should be noted that the size (i.e., inductance) of the sense loop of this probe will affect the amplitude of the measured voltages. Measured voltages and decision thresholds should be calibrated against both the probe geometry and rise-time, as well as the predicted voltages modeled in the various fault scenarios. Nominal test voltages for the A1 and A2 antennas are shown in Table 1.

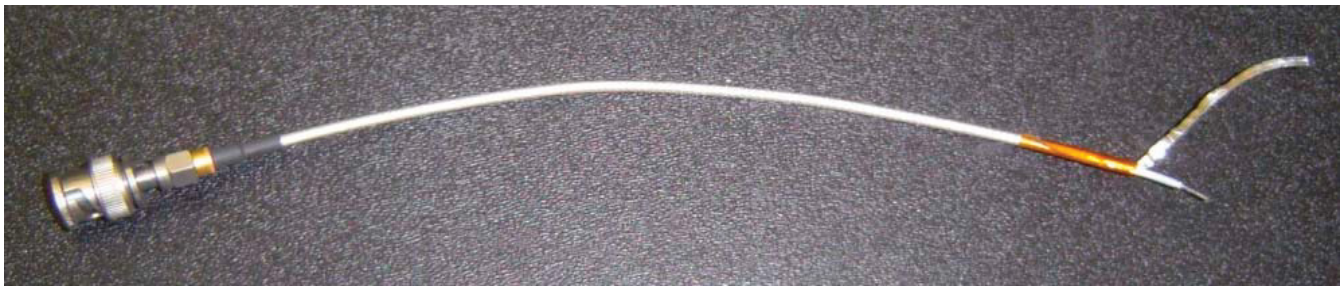

Figure 16 – Custom coaxial probe

The probe center conductor lightly contacts the lower corner of the patch (nearest the feed point) and the ground sheath touches the adjacent groundplane. The corner is chosen because it is generally easier to reach and either corner can be chosen for convenience. Precise attachment of the probe conductors is not required because this is not intended to be a precision measurement and hardware safety is the overriding concern. When a stable waveform is observed, the oscilloscope is stopped, freezing the waveform so that it can be observed and measured. The oscilloscope used for the A1 and A2 tests (TDS 3014B) has a built-in peak voltage measurement capability that can be used to display the peak-to-peak voltage. Waveforms that are anomalous (i.e., don't have the decaying exponential characteristic or have large amplitude deviations from nominal levels) can be recorded for further examination if necessary.

The pulse amplitudes are measured for each patch in turn and are recorded in Table 1. The data in the uppermost tables are nominal measurements for 'known good' A1 and A2 antennas. Each position in the matrix corresponds to a patch on the antenna. Generally speaking, the test results are within ±10% of the nominal values. The standard deviation between any particular measurement set and nominal set is 7.2mV for A1 and 3.5mV for A2. The peak deviations from nominal are with ±20% (20mV for A1 and 10mV for A2). These results are the basis for the ±50% threshold criterion for 'fault alarm'.

There is a noticeable taper to the amplitudes that is also symmetric. The corner element voltages are approximately 4.4dB lower for A1 and 2.7dB lower for A2 compared to the center element, whereas in-band, there is an 8dB difference. The difference in the impulse response tapers versus in-band taper can be attributed to the fact that the power dividing properties of the quarter wavelength Wilkinson circuits (designed for 600MHz for A1 and 1250MHz for A2) are less pronounced at 200MHz.

It is interesting to note that the post-acoustic test measurements for A1 are closer to nominal (and pre-test) than the intermediate post-thermal test measurements (1.9mV rms difference for former versus 7.2mV rms difference for latter). This is a natural consequence of the accuracy of the measurement technique and not a reflection of changes in the hardware. The variations can be attributed to minor differences in the probe attachment, including the inductance of the probe ground loop and placement of the operator's fingers at the attachment point. A more precise and repeatable attachment method could be devised to reduce the uncertainty of the measurement, but the current method provides acceptable accuracy relative to the aforementioned pass-fail criteria. Additionally, the current attachment method is quick and safe as it involves minimal contact with hardware. This also makes it suitable for in-situ measurement where access to hardware may be limited.

As mentioned earlier, the Impulse Test measurements should generally be performed in tandem with a return loss measurement, if possible. A comparison of measured return loss (reflection coefficient) is shown in Figure 17. These measurements generally agree with each other to within -25dB. It should be noted that for both A1 and A2, the 'before' measurements were made in an anechoic chamber and the 'after' measurements were made in JPL's Environmental Test Laboratory (ETL) High Bay. Room scattering is evident in the latter location and manifests as high-frequency ripples that are (for the ETL High Bay measurement) typically 1dB–2dB magnitude. Other scattering environments will obviously produce different results.

In summary, a test setup and procedure have been presented for measuring the impulse responses of the A1 and A2 antennas. The test involves the use of common electronic test equipment that is easy to configure and utilize – it takes about half an hour to conduct the test for a given antenna, including quality assurance checkpoints. This test provides a reliable 'health check' of the antennas with minimal risk to flight hardware. The measurements performed to date indicate that both the A1 and A2 antennas have not been adversely affected by environmental testing or handling.

Table 1 – Nominal and measured Impulse Test data

A1 Nominal (mV)				
100	120	130	120	100
105	135	155	135	105
110	140	165	140	110
105	135	155	135	105
100	120	130	120	100
A1 Pre-Thermal Test (mV)				
100	122	130	125	100
104	135	158	132	104
110	137	164	137	110
102	131	156	130	103
99	119	132	120	100
A1 Post-Thermal Test (mV)				
104	122	131	120	101
99	132	152	129	102
106	128	160	128	102
98	146	135	130	98
112	112	116	110	94
A1 Post-Acoustic Test (mV)				
103	120	131	120	103
105	132	154	134	106
108	137	166	140	108
103	132	151	133	106
100	119	127	117	101

A2 Nominal (mV)				
50	56	62	56	50
52	58	64	58	52
55	60	68	60	55
52	58	64	58	52
50	56	62	56	50
A2 Pre-Thermal Test (mV)				
53	61	62	58	52
51	56	67	60	50
52	60	67	55	55
54	58	66	52	54
52	57	62	57	50
A2 Post-Thermal Test (mV)				
47	55	60	56	51
51	58	65	64	52
53	61	65	62	51
51	58	61	62	51
47	56	60	57	50
A2 Post-Acoustic Test (mV)				
49	55	59	68	47
51	61	62	60	52
51	58	64	61	56
48	54	67	57	53
48	58	61	56	50

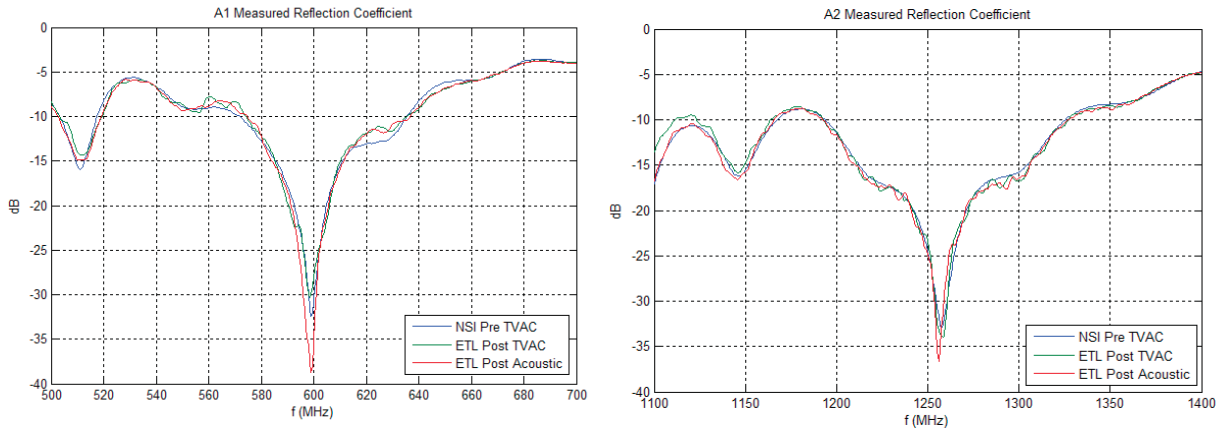

Figure 17 – Comparison of reflection coefficient measurements before and after thermal vacuum testing and acoustic testing for A1 (left) and A2 (right)

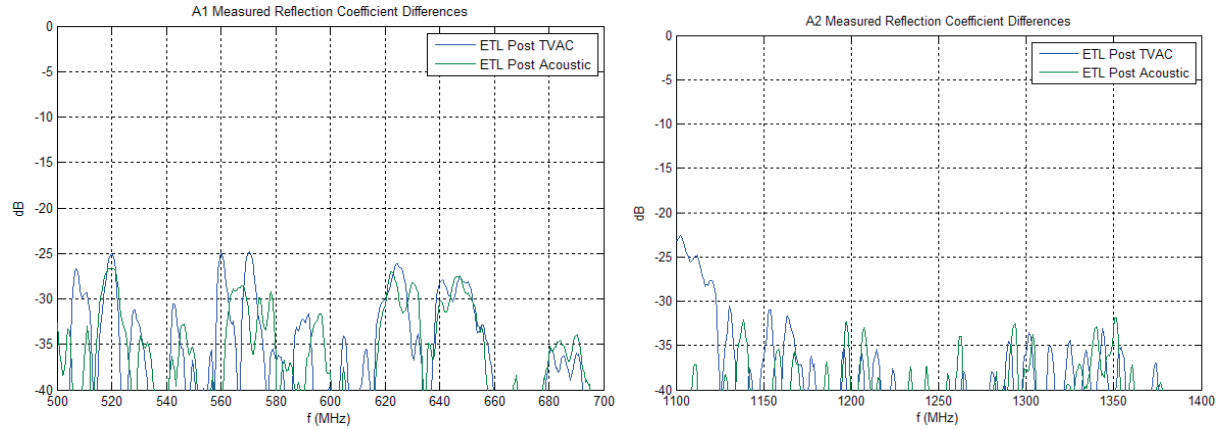

Figure 18 – Change in reflection coefficient after thermal vacuum testing and acoustic testing relative to pre-environmental test measurement (at NSI) for A1 (left) and A2 (right)

5. TIME-DOMAIN VERSUS FREQUENCY-DOMAIN

It is reasonable to consider the question of making the measurements discussed above in the frequency-domain. In principle, measurements can be made in the frequency-domain and transformed to the time-domain by the Fast Fourier Transform. The following section gives consideration to identifying fault conditions in the frequency domain alone. A vector network analyzer (VNA) could be used to measure the S-parameters of the feed network using a coaxial probe similar to the one shown in Figure 16 to connect the analyzer to the patch element. The key differences in the Impulse Test and a VNA measurement are summarized as follows.

First, the Impulse Test utilizes a baseband pulse, so it captures low frequency and DC information, whereas a VNA will always have a low frequency cut-off. This DC / low-frequency information can be important in detecting open circuits.

Second, in the time-domain Impulse Test method the total voltage at the antenna output is measured whereas an S-parameter measurement yields reflected to incident voltage ratio (S11) and transmitted to incident voltage ratio (S21). As the antenna and feed network are generally a bad match at low frequencies, S11 tends to be large and S21 tends to be small. This results in S21 being sensitive to small perturbations in the attachment configuration, raising the possibility of false alarms.

Third, while the S11 and S21 curves for different elements have grossly similar characteristics, the individual resonances differ. For example maximum S21 for center element occurs at 435MHz, whereas maximum S21 for edge element occurs at 355MHz (Figure 19). This makes the formulation of a pass-fail criterion more complicated and subject to error. While it is possible to process S-parameter data to yield total voltage and then transform it to the time-domain, this emulates the oscilloscope measurement without the benefit of the immediacy and intuitiveness that is afforded by the time-domain method.

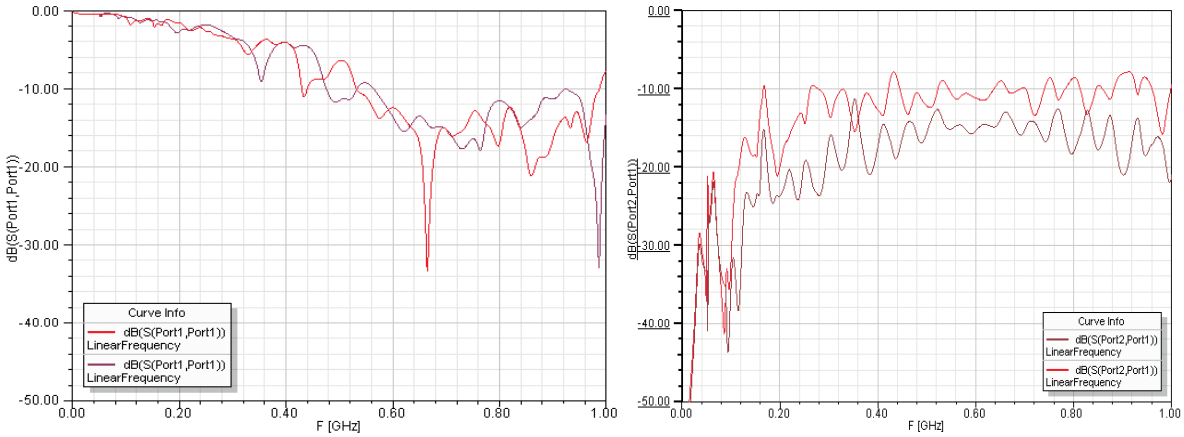

Figure 19 – S11 (left) and S21 (right) for two different elements: center element (red) and corner element (brown)

6. Limitations of Impulse Testing

Impulse Testing is intended to detect fairly catastrophic faults within the corporate feed network of patch array antennas that might not readily emerge from an impedance measurement. The repeatability of the test for a fault-free antenna, as elaborated in this paper, is typically within 10% and no worse than 20%. This makes the test less suitable for detecting more subtle faults, which necessarily have less impact on the impedance of paths within the feed network. Such faults could include a partially torn interconnect ribbon, or a broken but captured coaxial pin, for example. However, at the same time, it is questionable whether impedance measurements with a VNA or even pattern measurements could pick up subtle (non-catastrophic) faults in the antenna. It is quite likely that the precision of the measurements could be improved with improved probe and attachment approaches, but this would necessarily complicate the measurements

Impulse Testing, as elaborated here, relies on having a grounded patch in order to propagate a fast pulse from the rising edge of the applied pulse. A non-grounded patch configuration would require a faster pulse generator (pulse width on the order of a few ns) depending on the path length of the feed network. Alternatively, a grounding fixture could be applied to say the center of the patch to emulate the grounding mechanism of the support column of the metal patches presented here. These details would need to be incorporated into the circuit model when evaluating fault scenarios.

Impulse Testing depends on having good connectivity within the feed network to determine a baseline for fault-free measurements. It can accommodate variations due to manufacturing tolerances and workmanship as long as these are stable and are not issue-prone. As an example, some of the metal patches of the A2 antenna were not seated properly on the antenna groundplane owing to a tight clearance tolerance for the surface mount stud they attached to. A small air-gap under the foot of the metal patch base resulted in a small parasitic capacitance being introduced into the base impedance on an intermittent basis. As a consequence, the impedance of the component identified nominally as the inductor L4 in Figure 4 increased significantly, causing a large intermittent increase above nominal for the corresponding output voltage. This anomalous behavior, in tandem with visual inspection, was used to identify some of the affected patches and rework them before final testing. In this sense, Impulse Testing was used to identify a workmanship-related issue before final testing that was not discovered by routine visual inspection during assembly. However, the general conclusion is that unaddressed workmanship issues can confound subsequent downstream testing and should be avoided if possible. It is also interesting to note that RF performance was not impacted by the aforementioned workmanship issue, whereas Impulse Testing was affected by the workmanship issue.

7. Conclusions

A time-domain technique for testing the integrity of the corporate feed networks for the MWR A1 and A2 has been presented. The method relies on generating a low-frequency baseband pulse at the patch element and propagating it through the feed network to the antenna output, where it is measured with an oscilloscope. The method is easy to implement, fast, and can be done in confined environments that would otherwise preclude more conventional RF testing. Impulse Testing is proposed as a diagnostic tool for assessing the integrity of corporate-fed patch array antennas between environmental tests. Impulse Testing is not intended to replace precision microwave measurements, such as pattern testing and scattering parameter measurement, which are necessary to verify RF performance.

A circuit model for the A1 antenna, comprising lumped elements and lossy transmission lines, was developed and was found to show good agreement with measurements. The model was used to test a number of fault scenarios that may result from environmental testing or handling. While the fault testing was not exhaustive, the analysis showed that Impulse Testing is capable of detecting a broad range of likely faults, including open and short circuits in the interconnects, detached resistors, and even partially detached patch elements. These faults all represent fairly dramatic changes to the impedance of the feed circuit. More subtle changes to feed circuit configuration may not be as readily detected using this technique. This and other limitations of the technique were discussed.

Frequency-domain techniques were also considered for this test but were found to be less convenient and intuitive than the time-domain approach. A procedure and test setup for implementing the Impulse Test was presented, along with measurement data for the A1 and A2 antennas. Pass-fail criteria were formulated by testing various fault scenarios in the circuit model. This procedure was adopted as part of the test verification plan for the MWR antennas. Measured data taken before and after thermal testing and acoustic testing indicate that the antennas had not been adversely affected by environmental testing or handling.

The Impulse Testing method discussed in this paper was discussed for the specific case of the MWR patch array antennas. These antennas have a DC-coupled element and feature a fairly complicated transmission-line feed (also DC-coupled) with many interconnects. However, the technique has applicability, with minor modification, to other passive array configurations.

8. REFERENCES

[1] "Microwave Engineering 2nd Ed"., D.M. Pozar, Wiley 1998.

[2] "Inductance Calculations", F. W. Grover, Dover Publications, 2004.

[3] "Juno Microwave Radiometer Patch Array Antennas", N. Chamberlain, J. Chen, P. Focardi, R. Hodges, R. Hughes, J. Jakoboski, J. Venkatesan, M. Zawadzki, IEEE APS Conference, 2009.

[4] "The Juno Metal Patch Antenna Arrays", N. Chamberlain, J. Chen, R. Hodges, R. Hughes, J. Jakoboski, IEEE APS Conference, 2010.

9. BIOGRAPHIES

Neil Chamberlain *received the BSc. degree with Honours from Kings College London, UK in 1981. He worked briefly for Marconi Space and Defense Systems, Ltd., Portsmouth, UK before undertaking graduate studies at The Ohio State University, where he received the MS and Ph.D. degrees in Electrical Engineering in 1984 and 1989, respectively. He was a professor at the South Dakota School of Mines and Technology in Rapid City, South Dakota between 1990 and 2003. He taught courses in communication systems and electromagnetics, and his research focused on ultra-wideband radar antennas and systems. He is currently a Senior Engineer with JPL's Spacecraft Antennas Group, where he has delivered antenna arrays for the UAVSAR and Juno Microwave Radiometer instruments. Neil is currently leading the development of an array-fed reflector system for the DESDynI synthetic aperture radar instrument.*

10. ACKNOWLEDGMENTS

The research described in this paper was carried out at the Jet Propulsion Laboratory, California Institute of Technology, under a contract with the National Aeronautics and Space Administration.